AIP | Applied Physics Letters

Compositional instability in InAlN/GaN lattice-matched epitaxy

Q. Y. Wei, T. Li, Y. Huang, J. Y. Huang, Z. T. Chen et al.

Citation: Appl. Phys. Lett. **100**, 092101 (2012); doi: 10.1063/1.3690890
View online: http://dx.doi.org/10.1063/1.3690890
View Table of Contents: http://apl.aip.org/resource/1/APPLAB/v100/i9
Published by the American Institute of Physics.

Related Articles

High excitation carrier density recombination dynamics of InGaN/GaN quantum well structures: Possible relevance to efficiency droop
Appl. Phys. Lett. 102, 022106 (2013)

Strain assisted inter-diffusion in GaN/AlN quantum dots
J. Appl. Phys. 113, 034311 (2013)

Spin-filtering and rectification effects in a Z-shaped boron nitride nanoribbon junction
J. Chem. Phys. 138, 034705 (2013)

Electron mobility of ultrathin InN on yttria-stabilized zirconia with two-dimensionally grown initial layers
Appl. Phys. Lett. 102, 022103 (2013)

Band offset determination of mixed As/Sb type-II staggered gap heterostructure for n-channel tunnel field effect transistor application
J. Appl. Phys. 113, 024319 (2013)

Additional information on Appl. Phys. Lett.

Journal Homepage: http://apl.aip.org/
Journal Information: http://apl.aip.org/about/about_the_journal
Top downloads: http://apl.aip.org/features/most_downloaded
Information for Authors: http://apl.aip.org/authors

ADVERTISEMENT

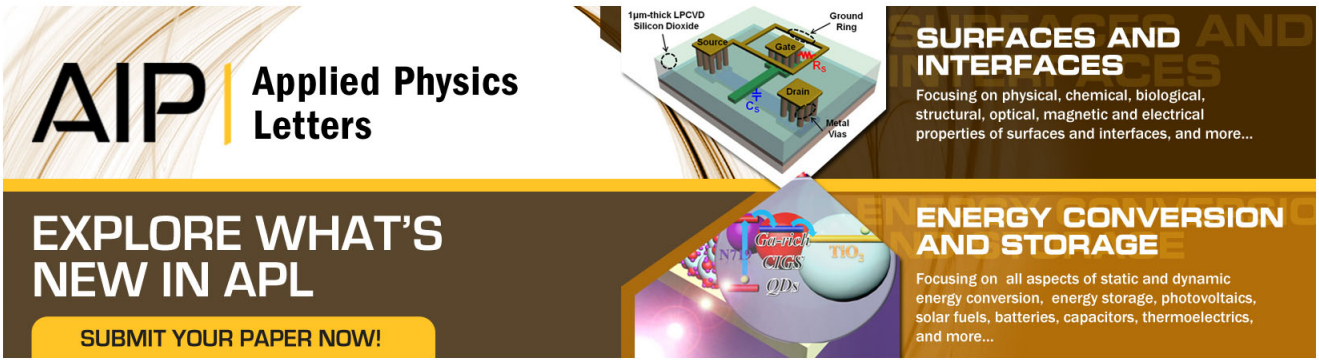

Compositional instability in InAlN/GaN lattice-matched epitaxy

Q. Y. Wei,[1] T. Li,[1] Y. Huang,[1] J. Y. Huang,[1] Z. T. Chen,[2] T. Egawa,[2] and F. A. Ponce[1,a)]
[1]*Department of Physics, Arizona State University, Tempe, Arizona 85287-1504, USA*
[2]*Research Center for Nano-Device and System, Nagoya Institute of Technology, Gokiso-Cho, Showa-Ku, Nagoya 466-8555, Japan*

(Received 14 January 2012; accepted 10 February 2012; published online 27 February 2012)

The $In_xAl_{1-x}N$/GaN system is found to show compositional instability at the lattice-matched composition ($x = 0.18$) in epitaxial layers grown by metal organic chemical vapor deposition. The breakdown in compositional homogeneity is triggered by threading dislocations with a screw component propagating from the GaN underlayer, which tend to open up into V-grooves at a certain thickness of the $In_xAl_{1-x}N$ layer. The V-grooves coalesce at ~200 nm and are filled with material that exhibits a significant drop in indium content and a broad luminescence peak. Transmission electron microscopy suggests that the structural breakdown is due to heterogeneous nucleation and growth at the facets of the V-grooves. © *2012 American Institute of Physics*. [http://dx.doi.org/10.1063/1.3690890]

Group III nitride materials are widely used in electronic and optoelectronic devices. In particular, the $In_xAl_{1-x}N$ alloys have recently received much attention for applications in thin film structures with $x \sim 18\%$, lattice matched to GaN. Minimizing the lattice mismatch is expected to provide better structural characteristics and the possibility of growing thick $In_xAl_{1-x}N$ layers for distributed Bragg reflectors and optical waveguides.[1,2] However, from previous studies of thick $In_xGa_{1-x}N$ films with $x \sim 0.20$, we should suspect InAlN alloy instability due to tendencies towards spinodal decomposition.[3,4] Compositional instabilities in InGaN/GaN and AlGaN/GaN systems have also been explained by a compositional pulling effect where, during the initial deposition of InGaN or AlGaN on GaN, the incorporation of In or Al atoms is impeded by lattice mismatch strain.[5,6] In this paper, we report the observation of compositional instability in thick InAlN epilayers grown on GaN, triggered by the presence of threading dislocations that produce V-shape pits, whose facets act as heterogeneous nucleation sites for growth with significant lower indium content.

The InAlN epilayers in this study were grown on GaN at ~800 °C by metal organic chemical vapor deposition using a Taiyo Nippon Sanso SR2000 system.[7] We have investigated the effect of thickness on the structural and optical properties of films grown under otherwise similar conditions. We observe an interesting transition in the microstructure of epilayers in the thickness range between 140 and 500 nm. The microstructure of the epilayers was studied by transmission electron microscopy (TEM), in a Philips CM200 instrument operating at 200 KV. The TEM specimens were prepared by mechanical wedge-polishing techniques, followed by ion milling in a cold stage in order to minimize indium diffusion. Cathodoluminescence spectra were obtained at near liquid-helium temperatures in a scanning electron microscope.

The chemical composition of the epilayers was determined using Rutherford backscattering spectrometry (RBS). The spectra of InAlN/GaN films with thickness 140 and 500 nm are shown in Fig. 1. The helium-scattering energies corresponding to aluminum and indium atoms are 1.105 and 1.741 MeV, respectively, and are identified in the figure with vertical lines. The spectral width for each atom is related to the epilayer thickness and is due to frictional energy losses as the He atom penetrates to a certain depth before being backscattered; thus the spectra provide a compositional depth profile of each atomic species. The composition values determined by RBS are not affected by strain and defects in the epilayer; hence, they are more accurate than conventional x-ray diffraction measurements, where Poisson-ratio effects need to be considered.[3] Analysis of the spectra shows that the 140-nm-thick InAlN layer has a uniform composition with indium content of ~18%. On the other hand, the

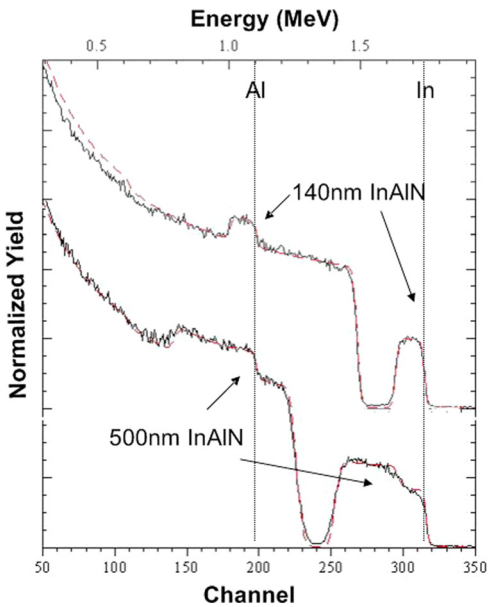

FIG. 1. (Color online) Rutherford backscattering spectra of InAlN epilayers with thickness of 140 and 500 nm. Solid lines are experimental data and dashed lines are simulated. The peaks corresponding to In and Al in the simulation indicate that the 140 nm epilayer has a uniform composition of $In_{0.18}Al_{0.83}N$, while the 500 nm epilayer consists of two sublayers, with $In_{0.10}Al_{0.90}N$ at the top and $In_{0.18}Al_{0.82}N$ at the bottom.

a)Electronic mail: ponce@asu.edu.

500-nm-thick epilayer consists of a uniform $In_{0.18}Al_{0.82}N$ layer followed by a region where the composition decreases linearly down to $\sim In_{0.10}Al_{0.90}N$.

We use cross-sectional TEM to understand the variation of composition in the thicker layer. Fig. 2 shows dark-field images for the 140 and 500 nm-thick InAlN samples. Under standard diffraction contrast, most of the dislocations are visible under $\boldsymbol{g} = [0002]$, indicating the predominance of screw and mixed dislocations, with Burgers vectors $\boldsymbol{c}$ and $\boldsymbol{c} + \boldsymbol{a}$, respectively, where $\boldsymbol{a}$ and $\boldsymbol{c}$ are the unit cell vectors in the hexagonal lattice.[8] A ratio of mixed to screw dislocations of $\sim$1:1 was found by diffraction contrast analysis. The image of the 140-nm-thick layer in Fig. 2(a) exhibits a relatively uniform contrast. There are only a few threading dislocations in the epilayer with an average density of $\sim 2 \times 10^9/cm^2$. Those dislocations open up at $\sim$80 nm above the InAlN/GaN interface. In the 500-nm-thick film in Fig. 2(b), it is observed that the defects rapidly increase beyond a thickness of $\sim$200 nm.

The microstructure of the 500-nm-thick epilayer can be observed in the bright-field TEM images in Fig. 3, which show the screw and edge components of the threading dislocations. These dislocations begin to open up laterally within the first $\sim$100 nm above the InAlN/GaN interface, forming a V-groove with a divergence angle of $\sim 36^\circ$, which is close to $\{1\bar{1}01\}$ facets. The beginning of similar openings is observed at the tip of some threading dislocations in the 140-nm-layer in Fig. 2(a). The fan-like regions originating from other dislocations in the vicinity but not contained in the thin TEM foil in Fig. 3 (of estimated cross-section thickness of $\sim$80 nm) coalesce at a distance of $\sim$200 nm from the InAlN/GaN interface. Microdiffraction from selected areas at the top of the film shows in Fig. 3(c) two distinct sets of diffraction spots. In the magnified region in the inset, we observe a small diffraction disk above a bigger disk. The small disk corresponds to the bottom region with uniform composition,

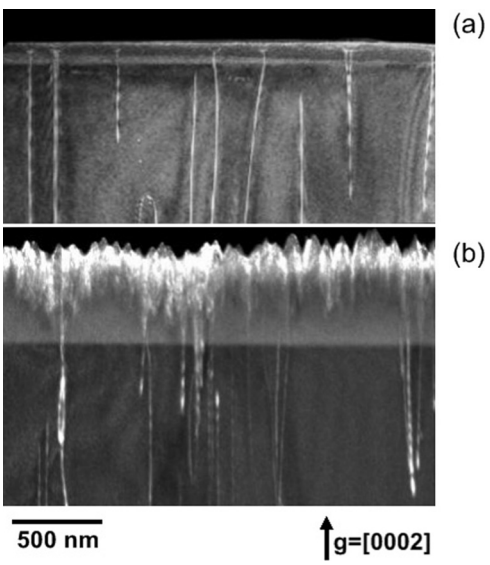

FIG. 2. Cross-section TEM dark-field images of InAlN epilayers grown on GaN, with thickness (a) 140 nm and (b) 500 nm. A relatively uniform layer contrast is observed in (a), but two sublayers with different contrast are observed in (b). Threading dislocations are observed to open at certain thickness in both figures.

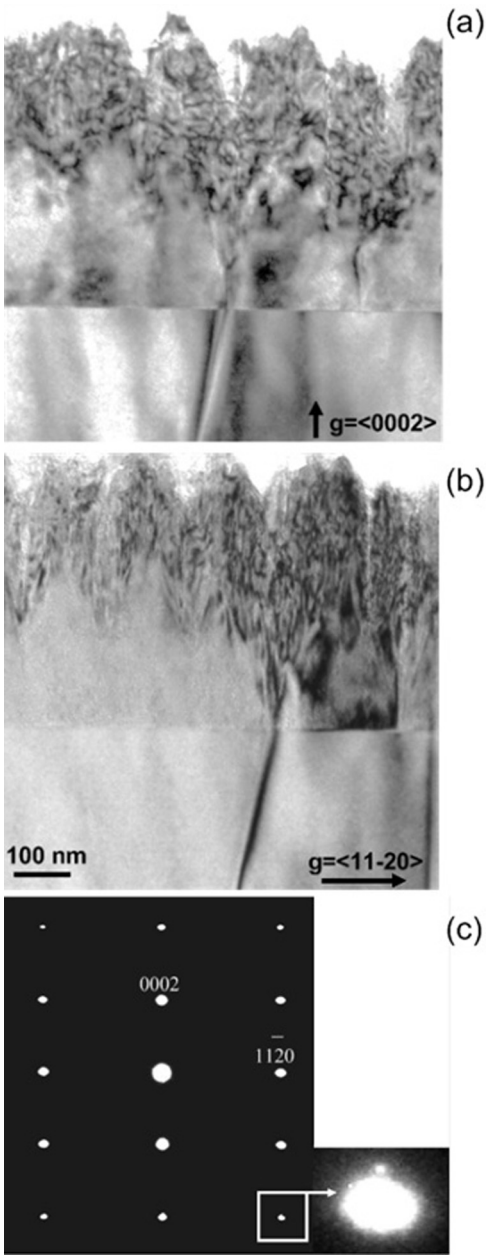

FIG. 3. Cross-section TEM bright-field images of 500 nm InAlN epilayers with (a) $g = [0002]$, (b) $g = [11\bar{2}0]$. (c) Selected area diffraction pattern of top region of the film.

while the larger disk corresponds to the top region of the film that constitutes the largest fraction of the area selected for diffraction. The large disk is elongated along the $[11\bar{2}0]$ axis reflecting reduced lateral dimensions of the crystallites responsible for this reflection. The large disk is displaced along the [0001] direction, indicative of the lower indium content in the top region. Thus, the compositional variation for thick InAlN layers can be summarized as follows. Initially, threading dislocations open up during growth due to the strain energy associated with the large Burgers vector, developing $\{1\bar{1}01\}$ facets.[9,10] We attribute the steady opening of the screw dislocations to local strain generated by random-alloy fluctuations. During subsequent growth, crystallites with an indium composition of $\sim$10% nucleate heterogeneously at the inclined facets of the open-core dislocations. The drop in indium content is clear from the RBS

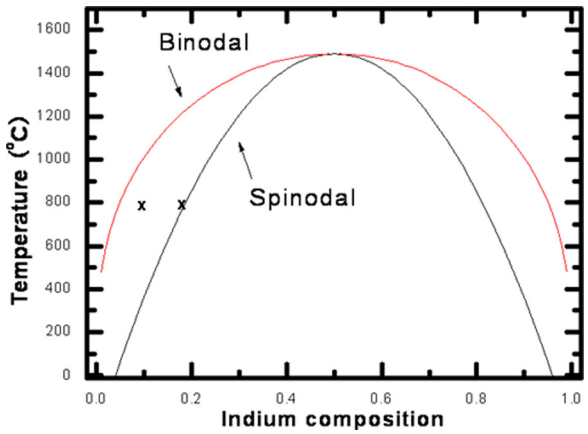

FIG. 4. (Color online) Spinodal and bimodal stability curves, calculated using an interaction parameter of 7.0 kcal/mole. The crosses indicate the compositions of the samples studied in this work, corresponding to x = 0.10 and 0.18.

data in Fig. 1 as well as from energy dispersive x-ray spectroscopy (EDS). No indium precipitates are detected. We suggest that the drop in indium content is related to growth on an inclined crystal plane. Or, more specifically, that compositional pulling leads to an Al-rich gas phase during c-plane growth, and that the presence of an inclined facet allows higher Al incorporation and an increase in growth rate. The crystallites that grow on the V-grooves resemble a columnar structure with diameters of ~15 nm, corresponding to a density of $\sim 5 \times 10^{11}/\text{cm}^2$. The final top surface reflects the V-groove morphology of the open-core threading dislocations. These observations in InAlN films are consistent with a model proposed by Northrup *et al.* for the formation of pits in GaN and its effect on In incorporation during growth of InGaN.[11]

The driving force for the compositional variation can be assessed from the phase diagram in Fig. 4. The solution model interaction parameter used in calculating this phase diagram is estimated from the lattice constant of InN and AlN, to be 7.0 kcal/mol.[12,13] The phase diagram shows the nature of the binodal and spinodal curves. The indium compositions observed in our samples (10% and 18%) are marked with crosses. At 800 °C, $In_{0.18}Al_{0.82}N$ is at the boundary between the metastable and unstable regions. Upon subsequent growth, the heterogeneous nucleation on the facet of hollow-core dislocations results in a phase with lower indium content and, from the phase diagram, with lower free energy.

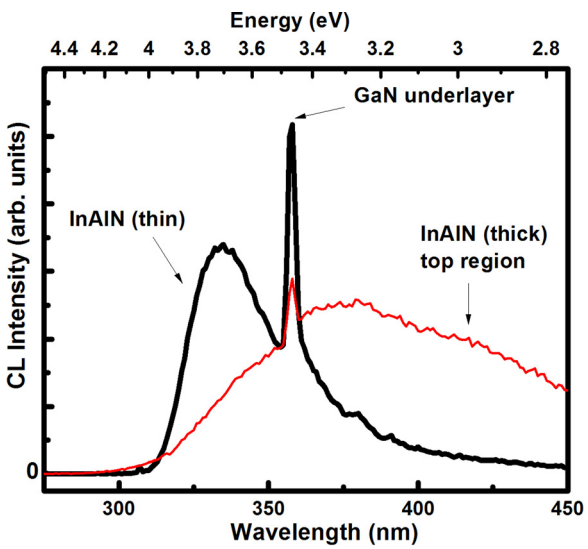

FIG. 5. (Color online) Cathodoluminescence spectra of InAlN epilayers with thickness of 140 and 500 nm. The InAlN emission becomes broader and red-shifted for the thicker film.

The optical characteristics of these layers can be assessed from the cathodoluminescence spectra in Fig. 5. The spectra were obtained with an electron accelerating voltage of 2.5 keV, which probes the near-surface region of the thin-film structures. In the case of the 140-nm-thick layer, the InAlN emission is centered at 3.74 eV (331 nm) with a FWHM of 0.30 eV; these values are similar to those reported by others.[2] The emission peak has anomalously low energies for the composition of the film, giving the impression of large Stokes-shift (of ~1 eV) or, alternatively, of a large bowing parameter (b > 10). The large Stokes-shift implies deep localization centers in InAlN, whose origin is still not clear.[14] For the 500-nm-thick layer, the broad emission of InAlN is probably due to the degraded crystal quality and/or to high densities of point defects.

In conclusion, compositional variations have been observed in thick InAlN epilayers. InAlN latticed-matched to GaN requires an indium content close to the miscibility gap at typical growth temperatures. The compositional instability is triggered by the presence of threading screw dislocations that open up into a faceted inverted pyramidal shape. InAlN crystallites with lower indium content nucleate heterogeneously on the facets of coreless dislocations. Two regions with distinct chemical composition and microstructural features are formed. The degraded crystal quality results in a defect-related broad optical emission.

[1]J. F. Carlin and M. Ilegems, Appl. Phys. Lett. **83**, 668 (2003).
[2]R. Butté, J.-F. Carlin, E. Feltin, M. Gonschorek, S. Nicolay, G. Christmann, D. Simeonov, A. Castiglia, J. Dorsaz, H. J. Buehlmann, S. Christopoulos, G. B. H. Von Högersthal, A. J. D. Grundy, M. Mosca, C. Pinquier, M. A. Py, F. Demangeot, J. Frandon, P. G. Lagoudakis, J. J. Baumberg, and N. Grandjean, J. Phys. D **40**, 6328 (2007).
[3]F. A. Ponce, S. Srinivasan, A. Bell, L. Geng, R. Liu, M. Stevens, J. Cai, H. Omiya, H. Marui, and T. Tanaka, Phys. Stat. Sol. B **240**, 273 (2003).
[4]V. G. Deibuk and A. V. Coznyi, Semiconductors **39**, 623 (2005).
[5]S. Pereira, M. R. Correia, E. Pereira, K. P. O'Donnell, C. Trager-Cowan, F. Sweeney, and E. Alves, Phys. Rev. B **64**, 205311 (2001).
[6]M. Hao, H. Ishikawa, T. Egawa, C. L. Shao, and T. Jimbo, Appl. Phys. Lett. **82**, 4702 (2003).
[7]Z. T. Chen, S. X. Tan, Y. Sakai, and T. Egawa, Appl. Phys. Lett. **94**, 213504 (2009).
[8]F. A. Ponce, D. Cherns, W. T. Young, and J. W. Steeds, Appl. Phys. Lett. **69**, 770 (1996).
[9]D. Cherns, W. T. Young, J. W. Steeds, F. A. Ponce, and S. Nakamura, J. Crystal Growth **178**, 201 (1997).
[10]D. Cherns, W. T. Young, J. W. Steeds, F. A. Ponce, and S. Nakamura, Philos. Mag. A **77**, 273 (1998).
[11]J. E. Northrup, L. T. Romano, and J. Neugebauer, Appl. Phys. Lett. **74**, 2319 (1999).
[12]I.-H. Ho and G. B. Stringfellow, Appl. Phys. Lett. **69**, 2701 (1996).
[13]J. A. Van Vechten, Phys. Rev. **182**, 891 (1969).
[14]S. Srinivasan, L. Geng, R. Liu, F. A. Ponce, Y. Narukawa, and S. Tanaka, Appl. Phys. Lett. **83**, 5187 (2003).